Supp. fig. 1-Cech

a

```
                 * * * ****** ***    ***  * **              *   **  *  * ******* * ** **  *   *
Human     91 GRLVLRPWIRELILGSETPSSPRAGQLLEVLQDAEAAVAGPSHAPDTSDVGATLLVSDGTHSVRCLVTREALDTS 165
Monkey     5 GRLVLRPWIRELILGSETLSSPRAGQLLEVLQEAEAAAAGPSHAPDASDVGATLLVSDGTYSVRCLVTREALDTS  79
Dog        5 GSLVLRPWIRELVLGSDALSSPQPGQLLEAEAQAQA--PGPPRVPDTSDVAAALLVSDGTHSVRCLVTREALNAS  77
Cow       36 GGLVLRPWIRELVLGSDALSSPRAGQLLKVLQEAKA--QSPSGAPDPPDAEAMLLVSDGTHSIRCLVTGEALNAS 108
Horse     59 GTLVLRPWIRELVLGSEALSSPRAGQLLEVLQDDEG--PGPSRAPDTPDVGAALLVSDGTYSVRCLVTREAVNTS 131
Mouse      5 GLLALQPWIRELILGSETLSSPRTGQLLKVLQDSET--PGPSSAPDTPDTGAVLLVSDGTHSVRCVVTRNAIDTS  77
Rat        5 GRLVLRPWIRELILGSETLSSPQAGHLLKVLQDSET--PGPSSAPDTPDTGAVLLVSDGTHSVRCVVTRNAIDTS  77

                    *** ** **** *** ***  *    **      ********** *******   * *** * **  **  *
Human             DWEEKEFGFRGTEGRLLLLQDCGVHVQVAEGGAPAEFYLQVDRFSLLPTEQPRLRVPGCNQDLDVQKKLYDC    237
Monkey            DWEEKEFGFRGTEGRLLLLQDCGVHIQVAEGGAPAEFYLQVDRFSLLPTEQPRLRVPGCNQDLDVQKKLYDC    151
Dog               DWEEKEFGFRGAEGRLLLLQDCGVRVQVGEGGAAAEFYLQVDRFSLLPTEQPLERVIGCNQDPDVQKKLFDC    149
Cow               DWEEKEFGFRGTEGRILLLRDCKVSVQVAQGDTPAEFYLQVDRFALLPTEQPREQVTGCNEDPDVRKKLCDC    180
Horse             DWEDKEFGFRGSEGRLLLLQDCDVRVQVAEGGAPAEFYLQVDRFSLLPTEQPRERVTGCNQDPDVQKKLYDC    203
Mouse             DWEEKELGFRGTEGRLLLLQACGLRVQVAQDHAPAEFYLQVDRFNLLPTEQPRIQVTGCNQDSDVQRKLNEC    149
Rat               DWEEKEFGFRGTEGRLLLLQACGLRIQVAQDYAPAEFYLQVDRFNLLPTEQPRVQVTGCNQDSDVQKKLNKC    149
```

b

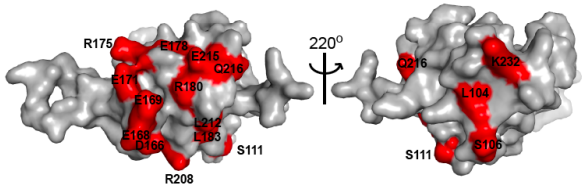

c

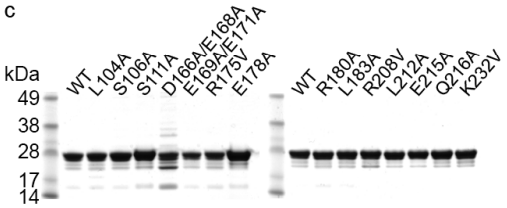

Supp. Figure 1. Site-directed mutagenesis of the surface of the N-terminal OB domain of TPP1. a, Amino acid sequence alignment of the OB domains of TPP1 proteins from indicated species is shown with fully conserved residues indicated with an asterisk. **b**, Two views of structure of the OB domain of TPP1 (PDB: 2I46) are shown in a grey surface representation with conserved surface residues (annotated in red in panel **a**) shown in red. **c**, Aliquots (4 µg) of wild-type (WT) and indicated mutants of TPP1 were analyzed by coomassie-stained SDS-PAGE. The positions and sizes (kDa) of marker polypeptides are indicated on the left.

Supp. fig. 2-Cech

a

TPP1	K_D (nM)
– (POT1 alone)	1.2
WT	0.38
L104A	0.30
S106A	0.24
S111A	0.21
D166A/E168A	0.28
E169A/E171A	0.28
R175V	0.27
E178A	0.25
R180 A	0.3
L183 A	0.27
R208V	0.37
L212A	0.5
E215A	0.41
Q216 A	0.31
K232V	0.28

b

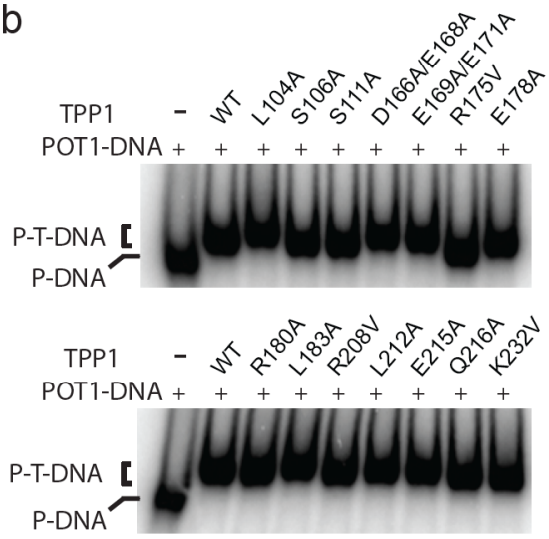

Supp. Figure 2. TPP1-OB surface mutants do not show defects in POT1-DNA binding. a, Filter-binding was used to quantify the affinities of the various TPP1 mutants for POT1-DNA. The data were plotted (main text Figure 1b) and analyzed using Kaleidograph (Synergy software) and fit using the equation: Fraction Bound = ([POT1]*m1/([POT1] + K_D) + m3). m1, m2, and K_D were optimized to obtain the best fit to the data. The calculated K_D values for the various POT1-TPP1-DNA complexes containing indicated TPP1 mutations are shown. The error in the K_D for experiments done in triplicate was <20% and identical trends were obtained in all individual experiments. **b**, EMSA of POT1-TPP1 with ^{32}P-labeled 20mer oligonucleotide of sequence $(dT)_8$GGTTAGGGTTAG. Binding mixtures contained 20 nM radiolabeled oligonucleotide, 200 nM POT1, and 400 nM of indicated TPP1 proteins. '-' indicates a binding reaction containing only POT1 and DNA. The positions of POT1-DNA (P-DNA) and POT1-TPP1-DNA (P-T-DNA) complexes are indicated on the left. The subtle differences in super-shifting by certain TPP1 mutants can be explained by the effect on electrophoretic mobilities of changes in charge associated with the respective mutations.

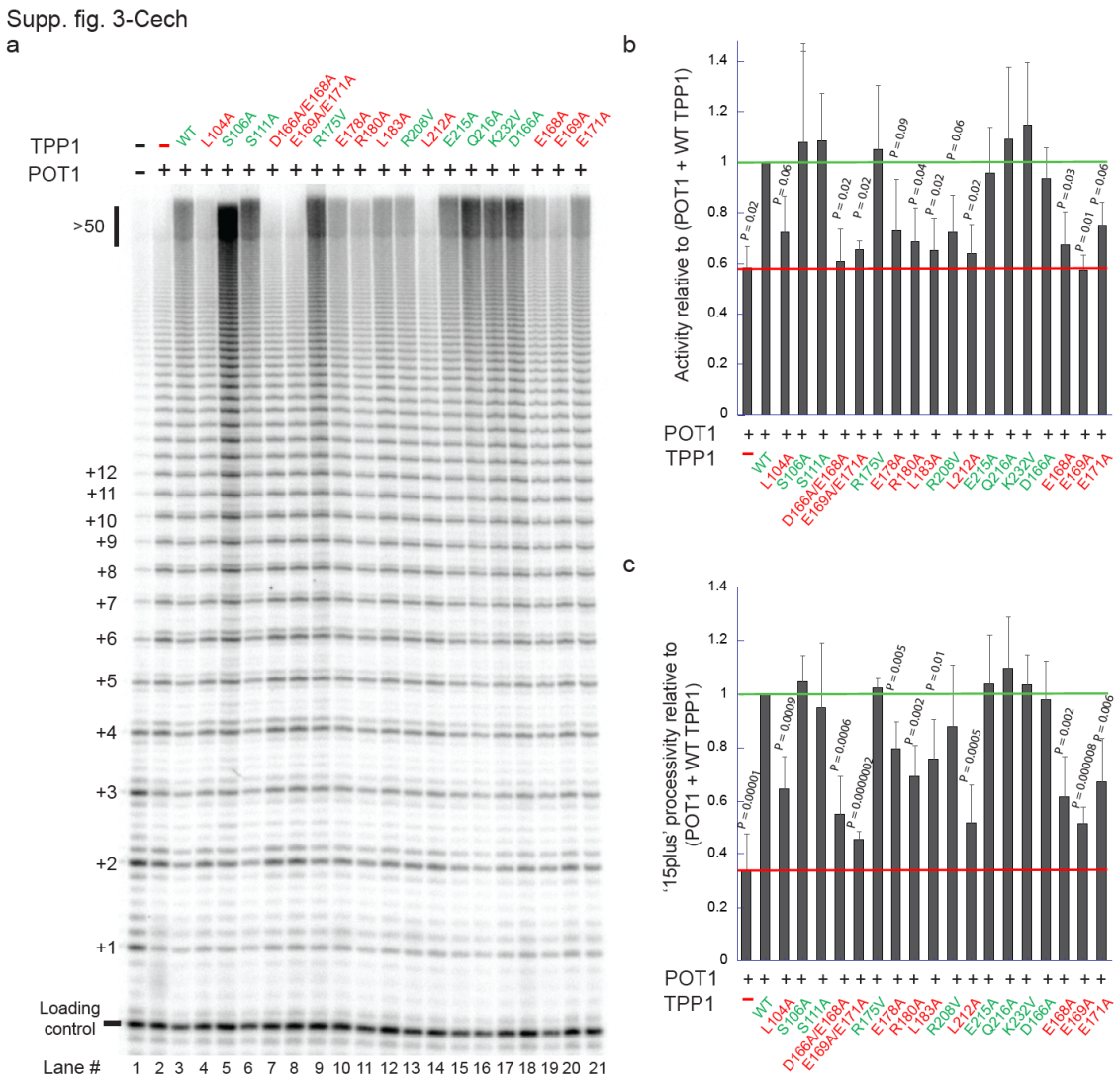

Supp. Figure 3. Several TPP1 OB mutants reduce the ability of POT1-TPP1 to enhance telomerase activity and processivity *in vitro*. a, Direct telomerase enzyme assays show the extension of primer a5 (50 nM) in the presence of POT1 (or absence of POT1: "-") and the indicated TPP1 proteins with super-telomerase from HEK 293T cell extracts. The number of telomeric hexad repeats added is indicated on the left. Qualitatively, the greater the intensity of high repeat number bands relative to low repeat number bands, the greater is the repeat addition processivity; the greater the total band intensity in a given lane, the greater is the activity. Mean total activity (panel **b**) and mean '15plus' repeat addition processivity (see Methods for definition) (panel **c**) relative to that of 'POT1 + WT TPP1' (green line) obtained from four independent sets of experiments (of which panel **a** is representative) are shown for the various TPP1 mutants along with error bars indicating standard deviations. Stimulation is assessed relative to the 'No TPP1' negative control (red line). P values from two-tailed Student's t-test are indicated above the bars in panels **b** and **c** for mutants showing statistically significant defects when compared to R175V, a mutant that behaves like wild-type. Mutants showing significant defects (P<0.09 in *b*, P<0.01 in *c*) are labeled in red and those not showing significant defects are labeled in green.

Supp. fig. 4-Cech

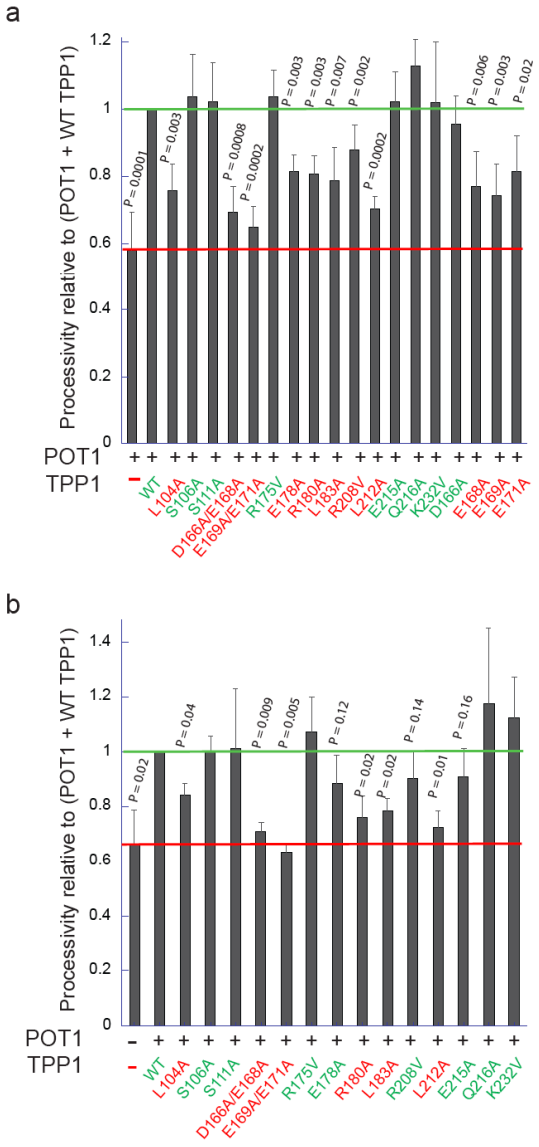

Supp. Figure 4. Repeat addition processivity quantification of data from gels shown in Supp. Figure 3a (panel a) and Figure 1c (panel b) using a previously reported procedure that involves quantification of individual bands in the ladder of telomerase products. Due to extensive band overlap from high telomerase processivity, individual contributions of upper bands in the gels are not used in this method. To accommodate the contributions of higher bands, the '15plus ' method described in the Methods was used (Figure 1d and Supp. Figure 3c). The green and red lines indicate levels for positive control (WT) and negative control (No TPP1), respectively. Mutants showing significant defects (P<0.02) are labeled in red and those not showing significant defects are labeled in green.

Supp. fig 5-Cech

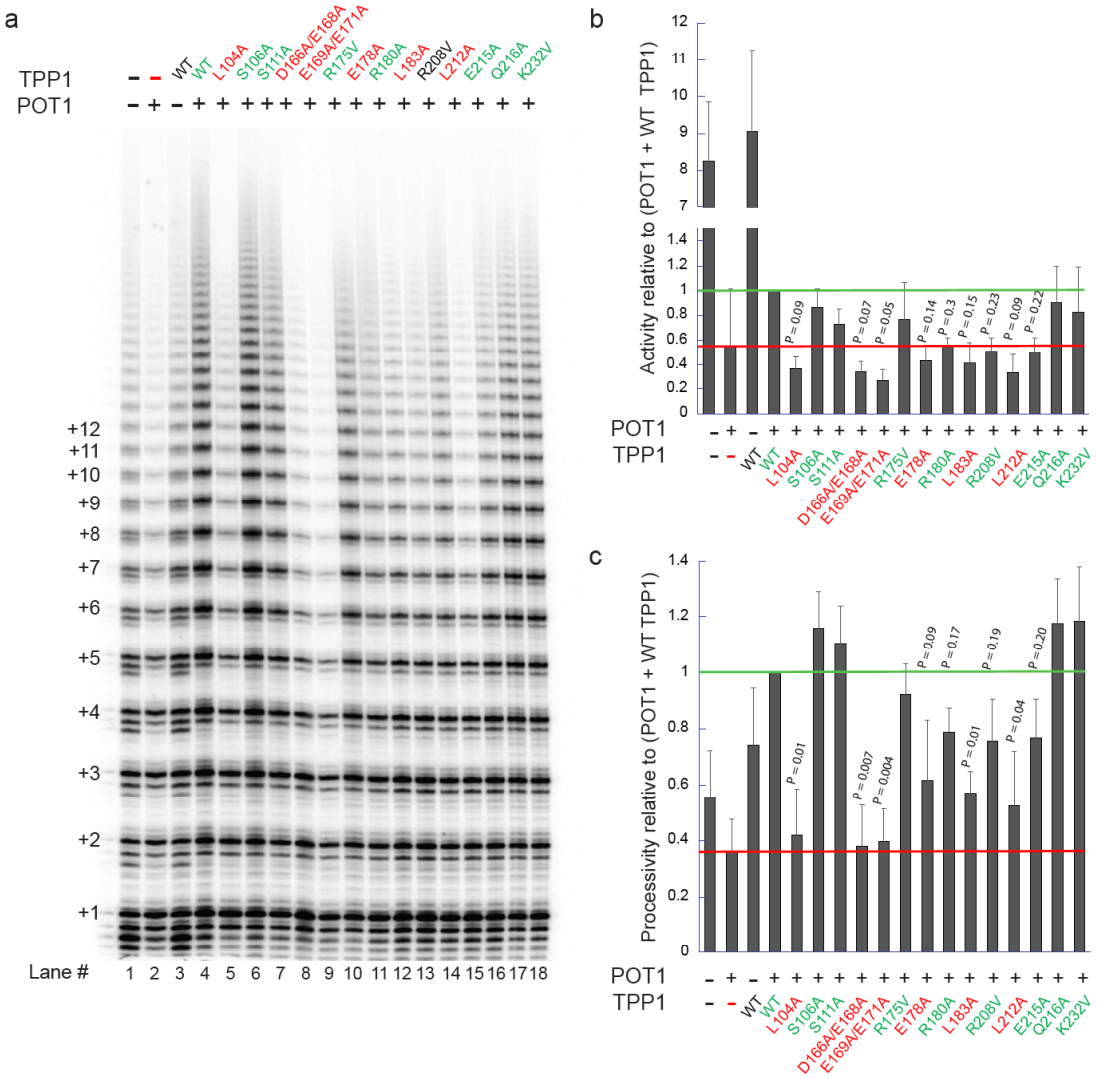

Supp. Figure 5. Effect of TPP1-OB mutations on the ability of POT1-TPP1 to enhance telomerase activity and processivity using primer $(GGTTAG)_3$. a, Direct primer extension assays including POT1 (or excluding POT1: "-") and indicated TPP1 proteins were performed with super-telomerase from HEK 293T cell extract using primer of sequence $(GGTTAG)_3$ (50 nM), also known as primer b. The number of telomeric hexad repeats added is indicated on the left. **b**, Mean total activity and **c**, mean repeat addition processivity (panel **c**) relative to that of POT1 + WT TPP1 (green line) obtained from three independent sets of experiments (of which panel **a** is representative) are shown for the various TPP1 mutants. Error bars, standard deviations. Stimulation of processivity is assessed relative to the 'No TPP1' negative control (red line). P values from two-tailed Student's t-test are indicated above the bars in (b) and (c) for mutants showing defects when compared to R175V, a mutant that behaves like wild-type. Mutants showing significant defects (P<0.15 in *b*, P<0.09 in *c*) are labeled in red and those not showing significant defects are labeled in green.

Supp. fig. 6-Cech

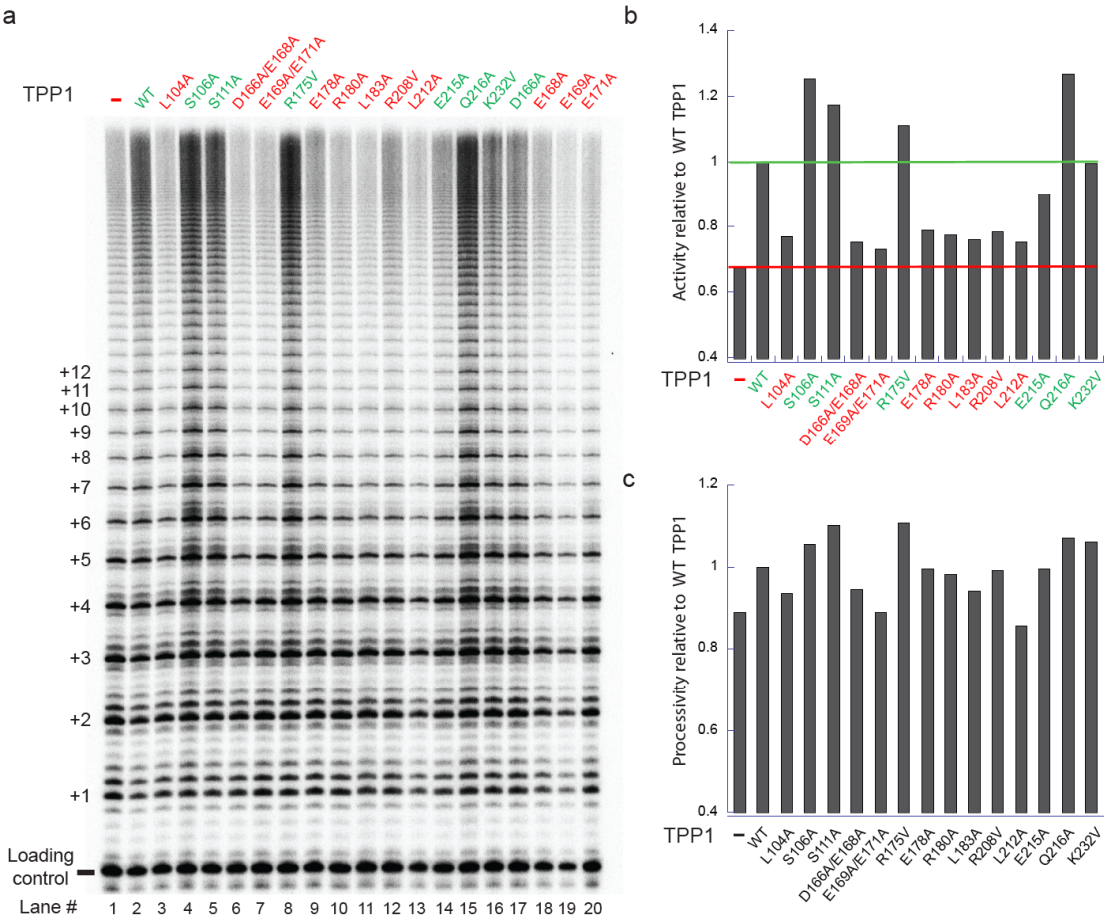

Supp. Figure 6. Wild-type TPP1 enhances telomerase activity in the absence of POT1 while several TPP1 OB mutants do not. a, Direct primer extension assays including indicated TPP1 proteins were performed with super-telomerase from HEK 293T cell extract using primer a5 (50 nM). The number of telomeric hexad repeats added is indicated on the left. **b**, Total activity normalized to the intensity of loading control relative to that of WT TPP1 is shown for the various TPP1 mutants. Green and red lines indicate levels for positive (WT) and negative (no TPP1) controls, respectively. Mutants showing defects (>75% reduction from green line towards baseline shown as red line) are labeled in red and those not showing defects are labeled in green. **c**, Repeat addition processivity, none of these effects were substantial.

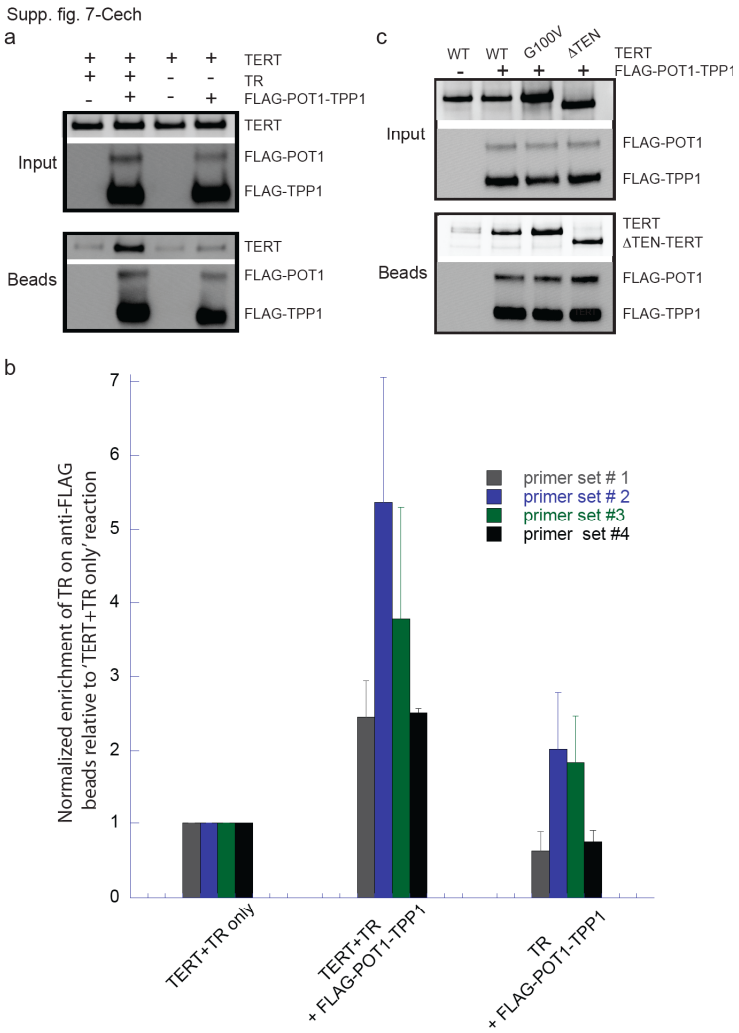

Supp. Figure 7. The TPP1-telomerase interaction requires TERT and TR but not the TERT-TEN domain. a and **c**, Pull-down of transiently expressed FLAG-TPP1, FLAG-POT1 and associated untagged TERT (or ΔTEN-TERT or G100V-TERT) from HeLa-EM2-11ht lysates on anti-FLAG conjugated beads. *Input*, immunoblot of soluble cellular lysates prior to incubation with beads. *Beads*, immunoblot of proteins retained on antibody beads after 2 h incubation at 4°C and washing. **b**, RNA-immunoprecipitation of transiently expressed TR on FLAG-POT1-TPP1 beads from lysates of formaldehyde-crosslinked HeLa-EM2-11ht cells also transfected with untagged TERT. The beads, after being washed with buffer containing 0.1% SDS, were treated with proteinase-K to elute bound RNA. The RNA eluate was reverse transcribed to cDNA and the amount of cDNA of TR was quantified using qPCR with four primer sets, each targeting a different region of TR. FLAG-POT1-TPP1 was omitted in the 'TERT+TR only' transfection, whereas TERT was omitted in the 'TR + FLAG-POT1-TPP1' reaction. The ratio of TR on beads versus in the input sample was calculated for each reaction and normalized to the 'TERT+TR only' control to yield 'Normalized enrichment of TR on anti-FLAG beads relative to 'TERT+TR' reaction' that is plotted along the Y-axis. Mean of three independent experiments is shown; error bars, standard deviations.

Supp. fig. 8-Cech

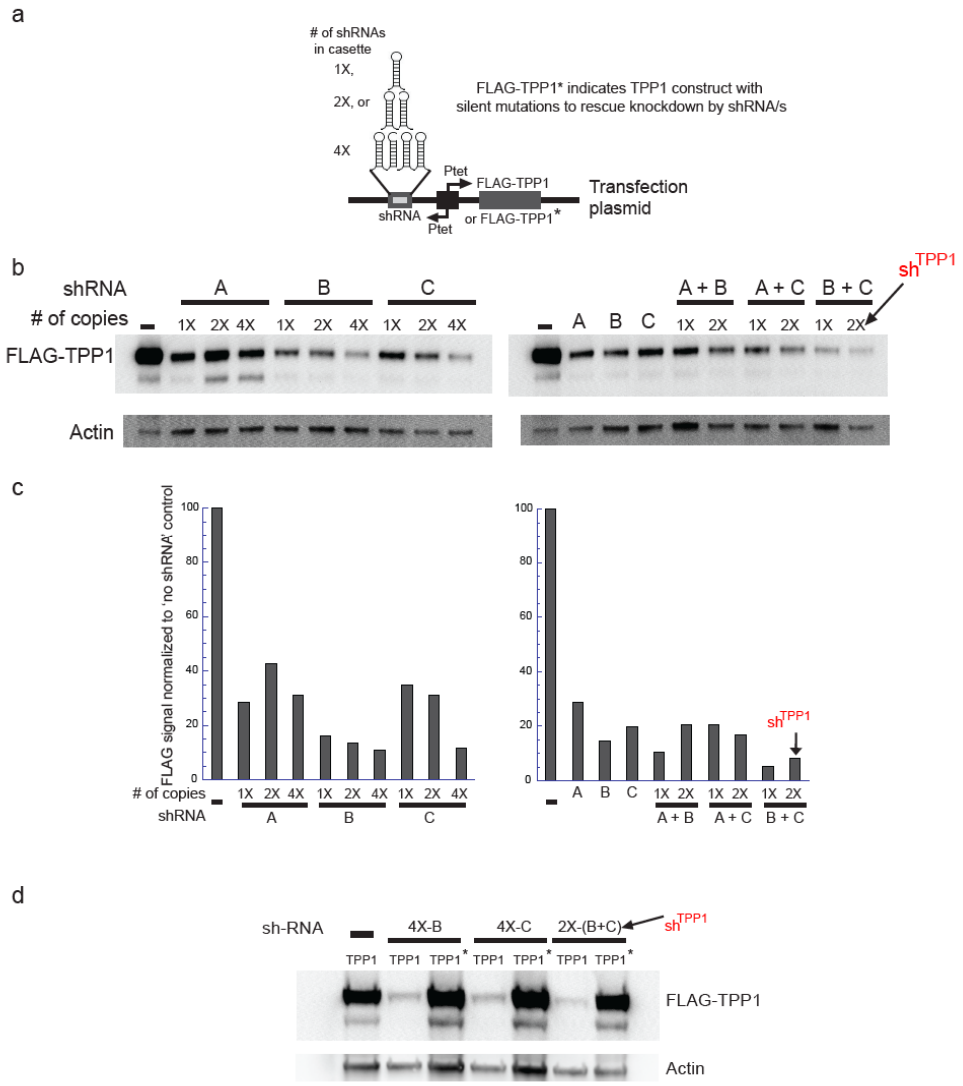

Supp. Figure 8. Screening for shRNA against TPP1 and rescue of knockdown using an shRNA-resistant version of WT TPP1. a, A bi-directional Tet-inducible vector encoding 1, 2 or 4 copies of shRNA genes of the same or different sequences in one direction and FLAG-tagged WT TPP1 in the other direction was used in transient transfection of HeLa-EM2-11ht to screen for RNA sequences that knockdown FLAG-TPP1 efficiently. **b**, Western blotting against the FLAG epitope showing that two (2X) or four copies (4X) of shRNA are more effective than a single copy (1X) in knocking down TPP1. The construct containing two copies each of shRNAs B and C is referred to as the sh^{TPP1} construct and was used in all experiments discussed in the main text that involve endogenous TPP1 knockdown (see Figure 3). **c**, Quantification of data shown in panel **b**. **d**, Silent mutations that do not change coding information were introduced into the target sites of indicated shRNAs on the TPP1 gene to engineer versions of WT TPP1 that are resistant to knockdown by these shRNAs.

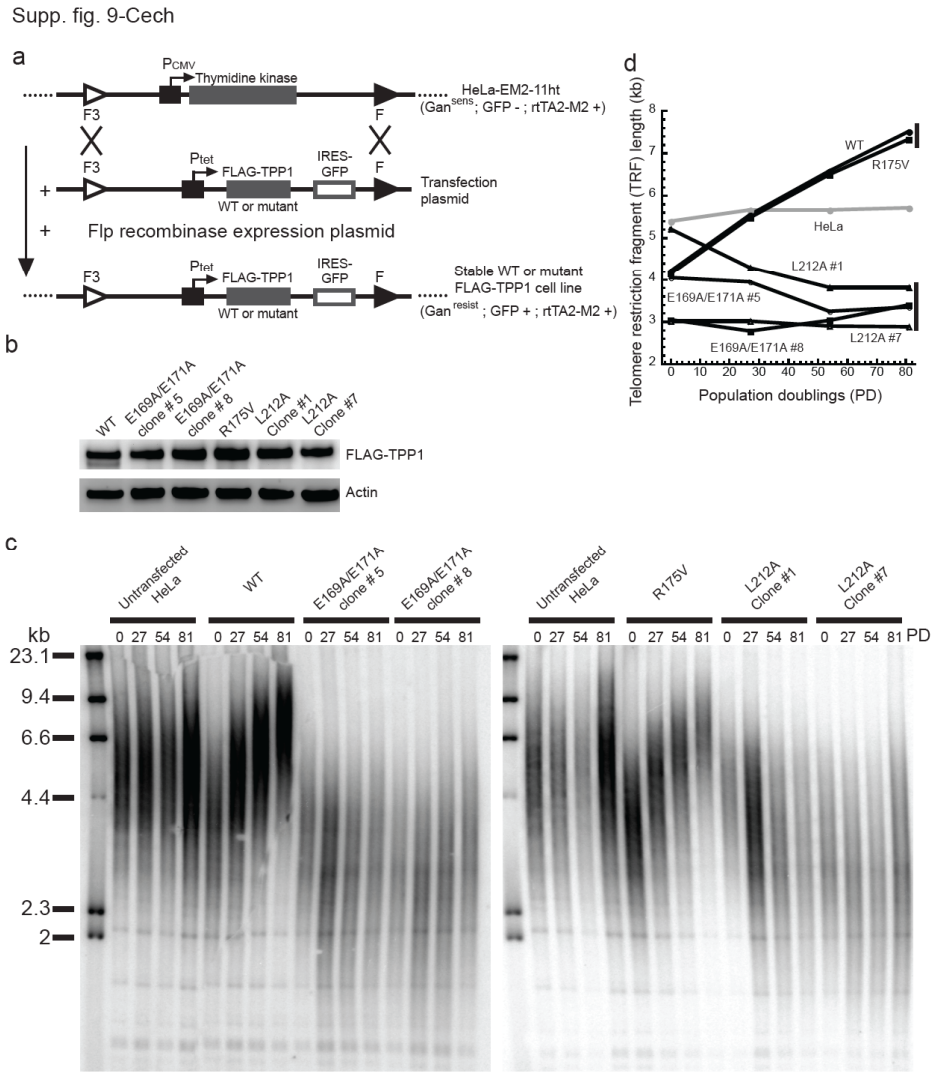

Supp. Figure 9. TPP1 TEL-patch mutants fail to stimulate telomere lengthening in human cells. a, Engineering HeLa-EM2-11ht stable cell lines containing a single-copy integration of Tet-inducible FLAG-TPP1 (WT or mutants) cassette and an IRES-GFP locus. The parent cell line constitutively expresses the reverse tetracycline-controlled transactivator (rtTA2-M2) allowing Tet-inducibility. Flp-mediated recombination promoted genomic integration of the cassette. Negative selection with gancyclovir eliminated un-recombined cells (Gan^{sens}) because they express thymidine kinase. Positive clones (Gan^{resist}) were screened for green fluorescence from the IRES-GFP locus after a 16 h doxycycline pulse (Supp. Fig. 8a,b). **b,** Immunoblot of stable cell lines showing comparable FLAG-TPP1 protein expression levels. **c,** Telomeric restriction fragment (TRF) Southern blot of HeLa-EM2-11ht (*Untransfected HeLa*) and stable cell lines expressing the indicated TPP1 constructs was performed at the indicated population doublings (PD). *Left lanes,* DNA length standards. **d,** The mean TRF length plotted against PD. The short bar indicates telomere length (~7 kb) attained by WT and R175V after 81 PD, whereas the tall bar indicates that the telomere length of E169A/E171A and L212A converge to 3-4 kb.

Supp. Fig. 10-Cech

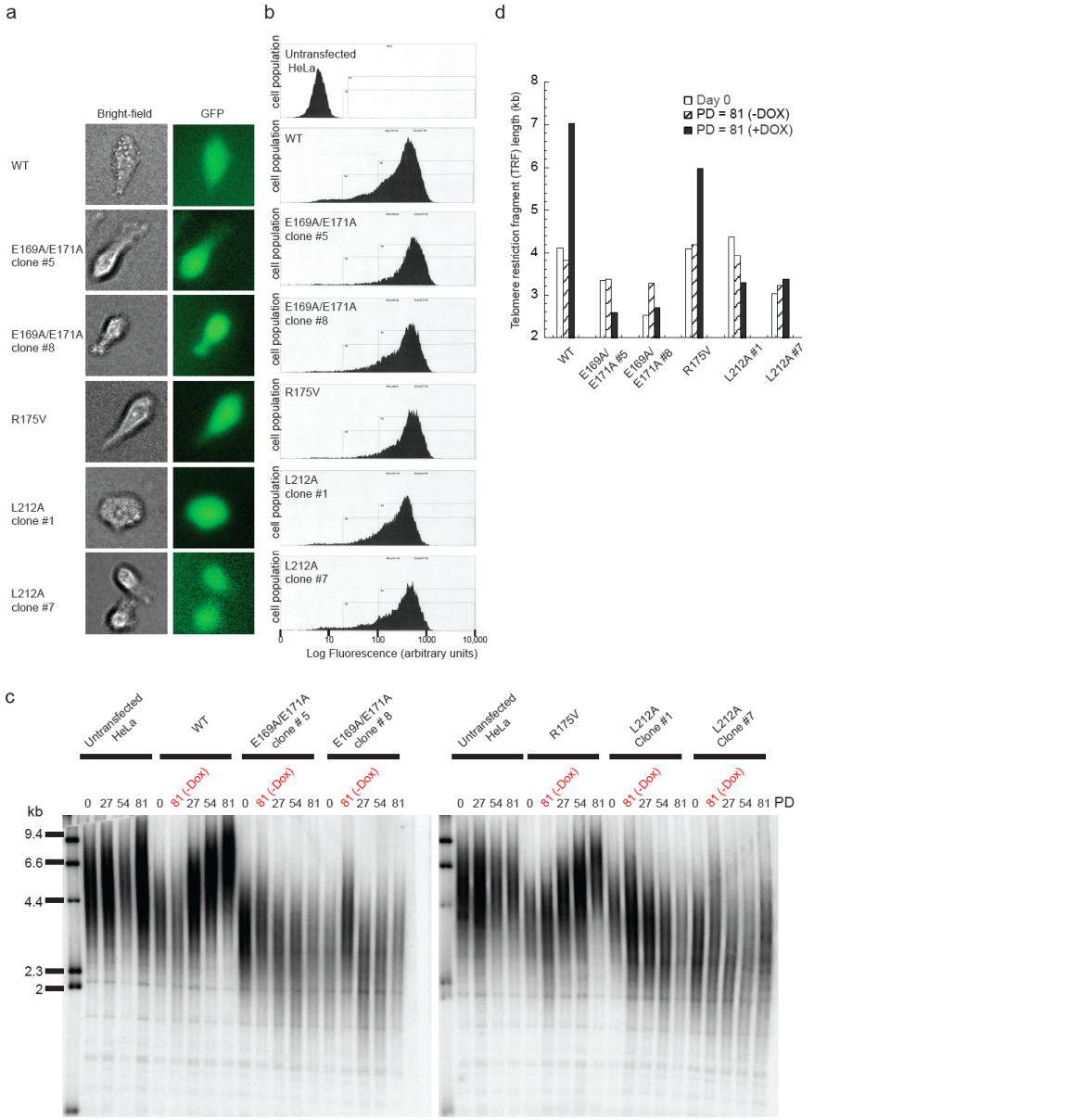

Supp. Figure 10. Screening, validation, and doxycycline-dependent telomere length analysis of cell lines with stable integration of TPP1 and GFP genes. a, GFP fluorescence and **b**, Flow cytometry analysis of stable clones of TPP1 also expressing GFP using an IRES locus present downstream of the TPP1 stop codon. **c**, Telomeric restriction fragment (TRF) Southern blot of stable cell lines expressing the indicated FLAG-TPP1 constructs was performed at the indicated population doublings (PD) for cells grown in the presence of doxycycline (200 ng/ml) (black labels) and in the absence of doxycycline (red label, '- Dox'). **d,** The mean TRF calculated for data shown in panel **c** was plotted for the various cell lines at the indicated PD. *Day 0:* time at which dox treatment was initiated; *PD = 81* (- Dox): 81 PD in absence of doxycycline; *PD = 81 (+ Dox)*: 81 PD in presence of 200 ng/ml doxycycline.

Supp. fig. 11-Cech.

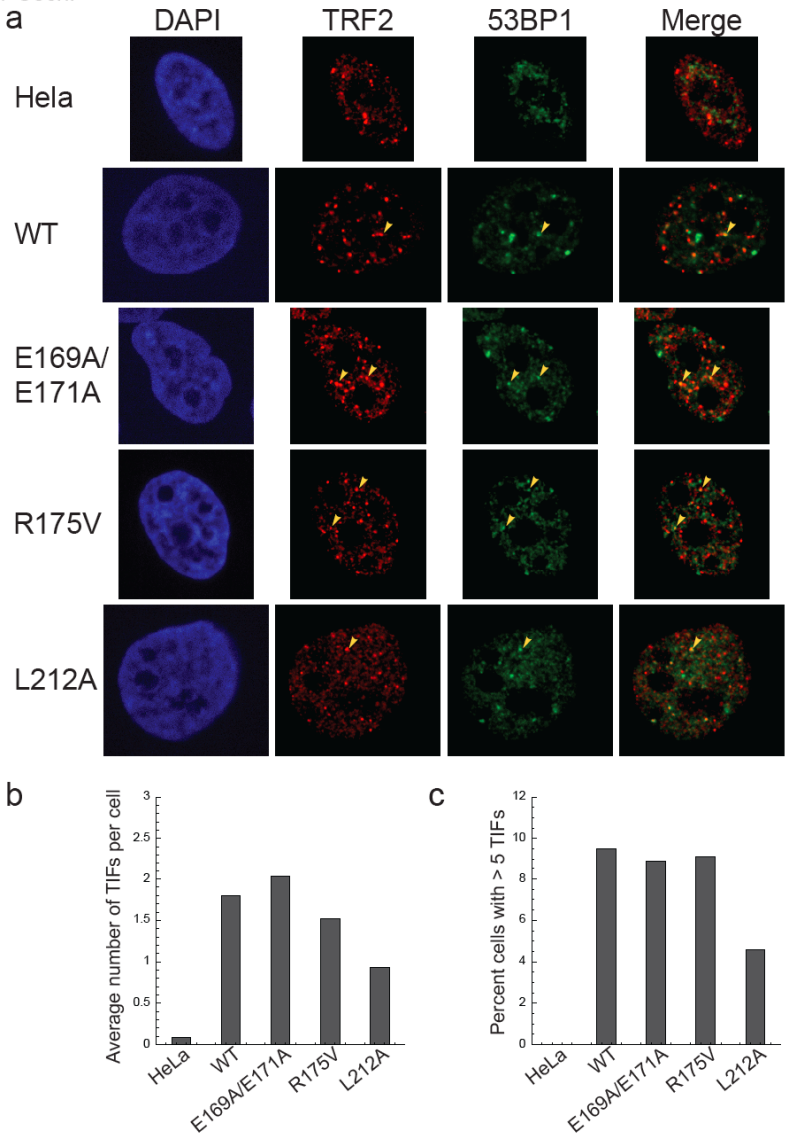

Supp. Figure 11. Telomere-dysfunction induced foci (TIFs) in stable cell lines expressing WT or mutant TPP1. a, Stable cell lines expressing WT or indicated mutant TPP1 proteins generated as described in Supp. Fig. 9a were subjected to co-immunofluorescence against TRF2 (telomere marker; red) and 53BP1 (DNA damage marker; green), and counterstaining with DAPI (blue). Colocalization of TRF2 and 53BP1 (yellow in merge) indicates DNA damage at telomeres or TIFs. **b**, Average number of TIFs/cell and **c**, % cells with greater than 5 TIFs were plotted for each of the indicated cell lines. 15 fields of view (40-120 cells) were used to obtain the plots shown in panels **b** and **c**. These data indicate that in general overexpression of TPP1 leads to moderate levels of TIF formation, but that the TPP1-OB mutations do not exacerbate this effect. We were unable to detect telomeric DNA with PNA-FISH probes in our HeLa cell lines. We reason that the short telomeres (3-5 kb including restriction nuclease-resistant sub-telomeric region) associated with these cell lines (see Supp. Fig. 9c) diminish the telomeric-FISH signal to levels below the background of detection.

Supp. fig. 12-Cech.

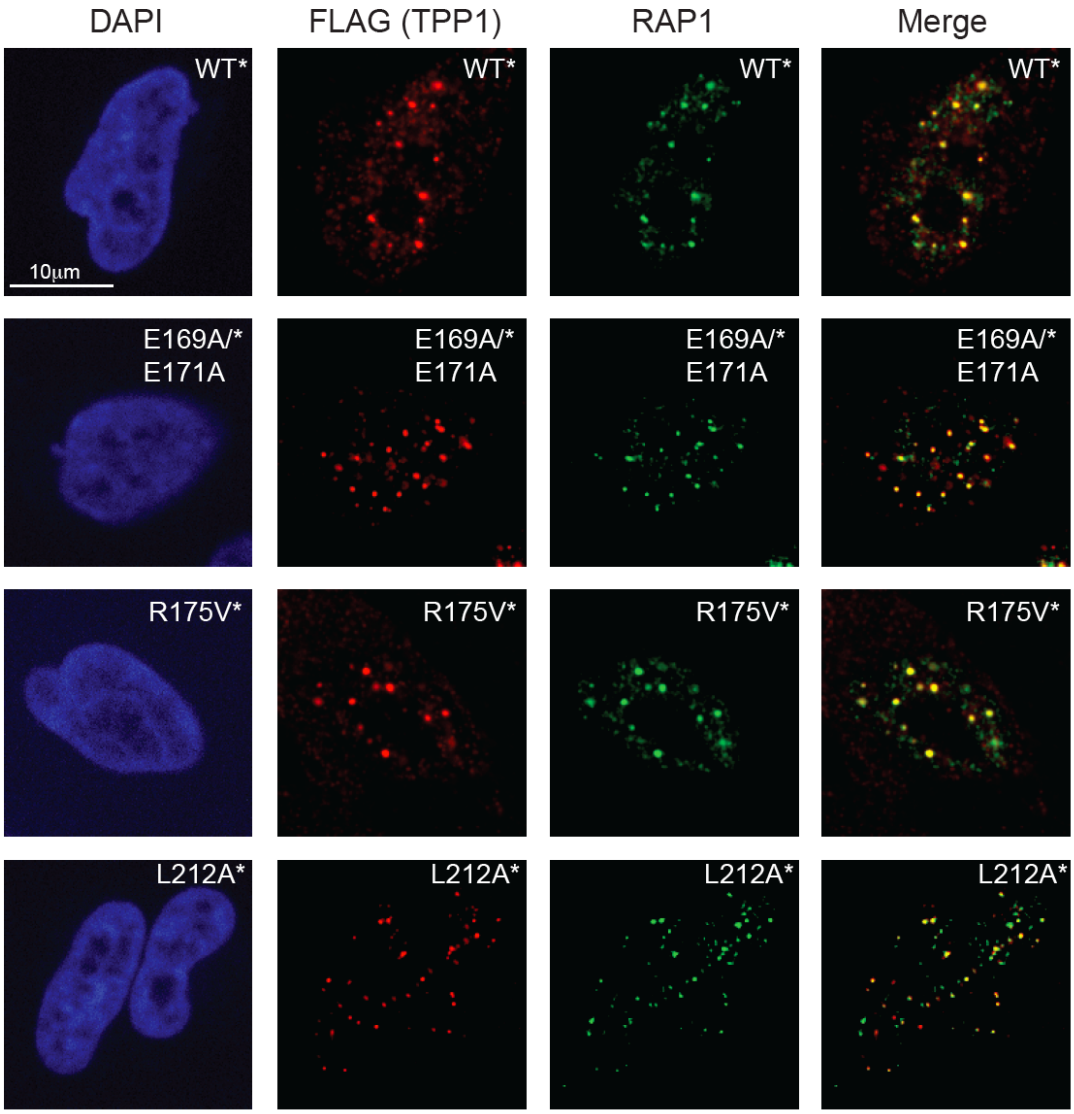

Supp. Figure 12. Wild-type and mutant FLAG-TPP1 proteins are localized at telomeres. Immunofluorescence to detect the recruitment of the indicated FLAG-TPP1 proteins (red) to telomeres (visualized with the shelterin component RAP1; green). *Merge*, Yellow spots indicate localization of FLAG-TPP1 at telomeres.

Supp. fig. 13-Cech

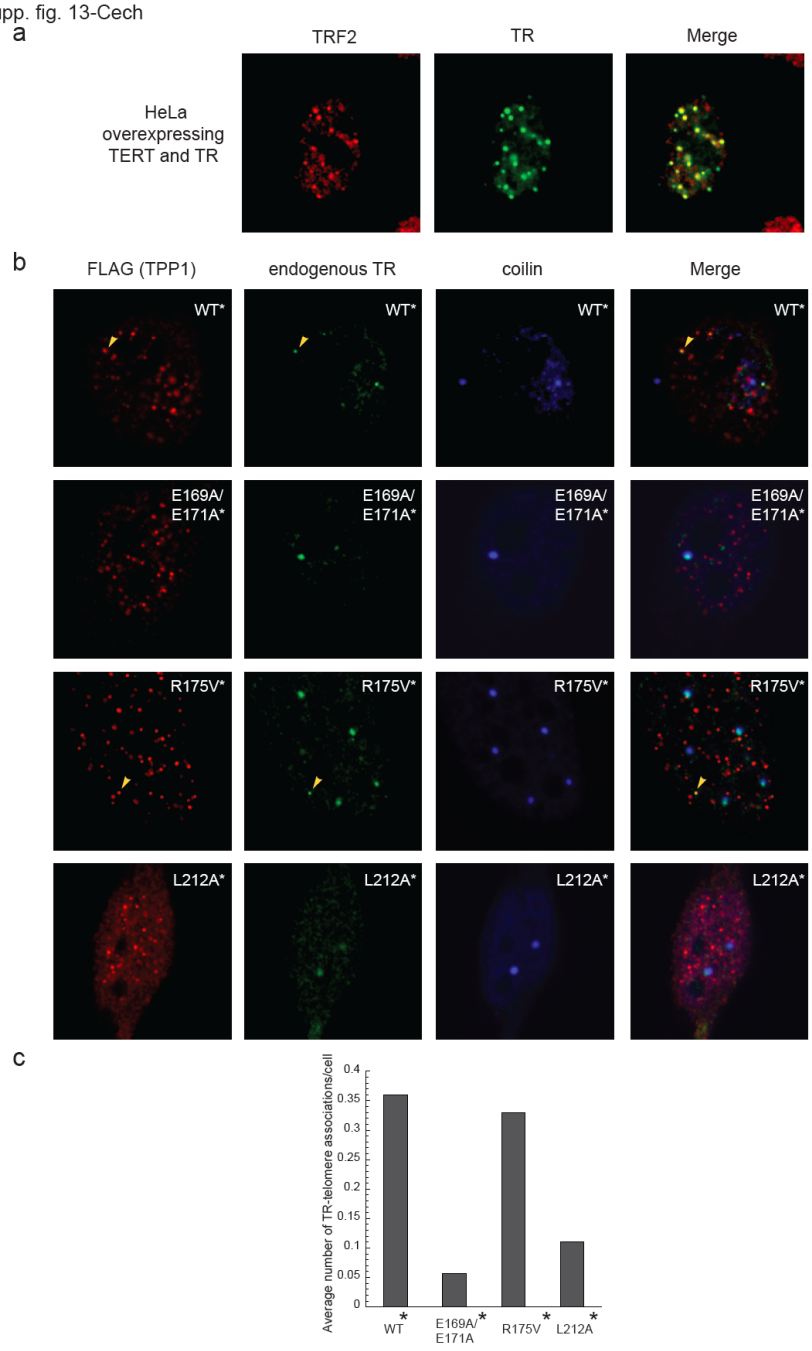

Supp. Figure 13. TEL patch mutants reduce recruitment of endogenous TR to telomeres. a, Overexpression of telomerase results in multiple TR foci (green) at telomeres (TRF2; red) even in the absence of FLAG-TPP1 overexpression. **b,** To assess endogenous telomerase recruitment in TEL patch mutant cells, the cell lines expressing the indicated TPP1 constructs but not overexpressing telomerase (untransfected cells) were synchronized using double thymidine block and analyzed by IF/FISH (as described in Fig. 4) after release of the cells into normal growth medium (+ 200 ng/ml doxycycline) for 4 h. **c,** Quantification of telomerase recruitment data. The average number of TR foci per cell (from 15 fields of view) is plotted for the indicated stable cell lines.

Telomerase recruitment in humans versus budding yeast

Unlike humans and *S. pombe*, budding yeast lack a shelterin-like complex and recruitment of telomerase in this organism occurs via i) interaction between the telomerase subunit Est1 and a budding yeast-specific ssDNA end-binding protein Cdc13[34-37] and ii) interaction between the telomerase RNA (called TLC1) and the Ku heterodimeric protein[38-41]. In addition, the telomerase regulatory Est3 subunit of budding yeast is predicted to fold into an OB domain that resembles TPP1-OB[42,43]. The similarity between Est3 and TPP1 could arise simply from them both being OB fold proteins[44]; alternatively, a recent study of the *Candida* Est3 proposes it to be functionally analogous to TPP1[45]. Amino acids E114/T115/N117 in *S. cerevisiae* Est3 have been found to bind to the TEN domain of Est2 (the *S. cerevisiae* TERT) and to stimulate telomerase activity[46]. However, It is difficult to compare these Est3 amino acids to the TEL patch, due to very limited sequence conservation between TPP1-OB and Est3 (~2% identity) and the absence of an Est3 structure.

Supplementary References

34 Nugent, C. I., Hughes, T. R., Lue, N. F., and Lundblad, V., Cdc13p: a single-strand telomeric DNA-binding protein with a dual role in yeast telomere maintenance. *Science* **274**, 249-252 (1996).

35 Qi, H. and Zakian, V. A., The Saccharomyces telomere-binding protein Cdc13p interacts with both the catalytic subunit of DNA polymerase alpha and the telomerase-associated est1 protein. *Genes Dev* **14**, 1777-1788 (2000).

36 Evans, S. K. and Lundblad, V., Est1 and Cdc13 as comediators of telomerase access. *Science* **286**, 117-120 (1999).

37 Pennock, E., Buckley, K., and Lundblad, V., Cdc13 delivers separate complexes to the telomere for end protection and replication. *Cell* **104**, 387-396 (2001).

38 Stellwagen, A. E., Haimberger, Z. W., Veatch, J. R., and Gottschling, D. E., Ku interacts with telomerase RNA to promote telomere addition at native and broken chromosome ends. *Genes Dev* **17**, 2384-2395 (2003).

39 Fisher, T. S., Taggart, A. K., and Zakian, V. A., Cell cycle-dependent regulation of yeast telomerase by Ku. *Nat Struct Mol Biol* **11**, 1198-1205 (2004).

40 Gallardo, F. et al., TLC1 RNA nucleo-cytoplasmic trafficking links telomerase biogenesis to its recruitment to telomeres. *EMBO J* **27**, 748-757 (2008).

41 Pfingsten, J. S. et al., Mutually exclusive binding of telomerase RNA and DNA by Ku alters telomerase recruitment model. *Cell* **148**, 922-932 (2011).

42 Lee, J. et al., The Est3 protein associates with yeast telomerase through an OB-fold domain. *Nat Struct Mol Biol* **15**, 990-997 (2008).

43 Yu, E. Y., Wang, F., Lei, M., and Lue, N. F., A proposed OB-fold with a protein-interaction surface in Candida albicans telomerase protein Est3. *Nat Struct Mol Biol* **15**, 985-989 (2008).

44 Lee, J. et al., Investigating the role of the Est3 protein in yeast telomere replication. *Nucleic Acids Res* **38**, 2279-2290 (2010).

45 Yen, W. F., Chico, L., Lei, M., and Lue, N. F., Telomerase regulatory subunit Est3 in two Candida species physically interacts with the TEN domain of TERT and telomeric DNA. *Proc Natl Acad Sci U S A* **108**, 20370-20375 (2011).

[46] Talley, J. M. et al., Stimulation of yeast telomerase activity by the ever shorter telomere 3 (Est3) subunit is dependent on direct interaction with the catalytic protein Est2. *J Biol Chem* **286**, 26431-26439 (2011).